Journal of the Korean Crystal Growth and Crystal Technology
Vol. 29, No. 3 (2019) 107-114
https://doi.org/10.6111/JKCGCT.2019.29.3.107

p-ISSN 1225-1429
e-ISSN 2234-5078

Study on simultaneous heat and mass transfer during the physical vapor transport of Hg_2Br_2 under μg conditions

Geug Tae Kim†

Department of Advanced Materials and Chemical Engineering, Hannam University, Daejeon 34054, Korea

(Received May 22, 2019)
(Revised June 3, 2019)
(Accepted June 3, 2019)

Abstract A computational analysis has been carried out to get a thorough and full understanding on the effects of convective process parameters on double-diffusive convection during the growth of mercurous bromide (Hg_2Br_2) crystals on earth and under μg conditions. The dimensional maximum magnitude of velocity vector, $|U|_{max}$ decreases much drasticlly near Ar = 1, and, then since Ar = 2, decreases. The μg conditions less than 10^{-2} g make the effect of double-diffusion convection much reduced so that adequate advective-diffusion mass transfer could be obtained.

Key words Double diffusion, Physical vapor transport, Vapor growth, Hg_2Br_2

1. Introduction

During the past 50 years one area of interest in natural convection research has been the study in confined geometries-enclosures. Examples of the enclosures may be parallelograms, three-dimensional enclosures, spheres or concentric annuli. In particular, one of the important topics in material processing is the growth of crystals in a sealed chamber as discussed by Osrtarch [1]. Crystal species was transported inside a closed tube from a source solid material at high temperature region to the growing crystal at low temperature region. The driving potential for the transport of crystal species was a temperature difference from the source interface at the high temperature region to the crystal interface at the low temperature region, which the equilibrium composition of the gas mixture is moved between the two ends and, thus, generated a concentrated gradient. In gravitational fields the simultaneous occurrence of temperature and concentration gradients would lead to double diffusion convection [2].

Kim and his coworkers [3-29] have systematically performed numerical studies of natural convection in the vapor phase during physical vapor crystal growth. Duval [30] reported that there exist four flow structure regions. During the change from one region to another region, three distinct bifurcation phenomena occur. The flow field structure shifts from a unidirectional advective-diffusion flow to two convection rolls, subsequently to four convection rolls, and finally six convection rolls. Singh et al. [31, 32] and Amarasinghe et al. [33] have studied the mercurous halide materials have proved to be most promising materials in applications for acousto-optic materials and signal processing optics such as Bragg cells.

In order to control the final quality of crystal affected by convection fields, it is required to study double diffusion convection flow structure in the vapor phase. In the author's previous results [34], the relations of aspect ratio and total molar flux was addressed and as a sequential study, in this paper the maximum magnitudes of velocity vector in the dimensional unit (cm/s) as a basis of convection intensity would be discussed with (1) aspect ratios, (2) Peclet numbers, (3) the driving potentials of the temperature differences between two ends in closed ampoules. A mixture of Hg_2Br_2 and argon is chosen as a systematic model both on earth and under μg environments, and a gravity vector of 10. Therefore, as a sequential study, in this paper one investigates numerically the characteristics of the double diffusion convection flow fields during the PVT processes of Hg_2Br_2 crystal growth.

2. Modeling

A steady state double diffusion convection in PVT crystal growth enclosure is considered with linear temperature profiles at sidewall boundary conditions, as

†Corresponding author
E-mail: geugtaekim@gmail.com

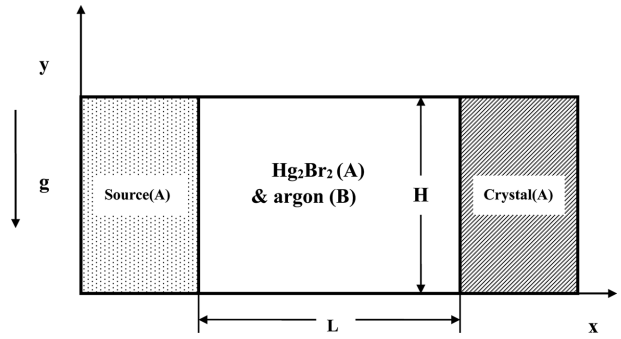

Fig. 1. Schematic and coordinates for modeling and simulation of PVT crystal growth reactor of Hg_2Br_2(A)-argon(B).

plotted in Fig. 1. The detailed assumptions can be found in reference [34]. u_x, u_y symbolize the x- and y-component velocity along the x- and y-coordinates in the rectangular coordinate system (x, y), respectively and T, ω_A, p stand for the temperature, mass fraction of species Hg_2Br_2 and pressure, respectively [34]. The superscript of * represents non-dimension state. The dependent variables appearing the governing equations are non-dimensionalized using the following groupings,

$$x^* = \frac{x}{H},\ y^* = \frac{y}{H}, \tag{1}$$

$$u = \frac{u_x}{U_c},\ v = \frac{u_y}{U_c},\ p = \frac{p}{\rho_c Uc^2}, \tag{2}$$

$$T^* = \frac{T - T_c}{T_s - T_c},\ \omega_A^* = \frac{\omega_A - \omega_{A,c}}{\omega_{A,s} - \omega_{A,c}}. \tag{3}$$

By applying the non-dimensional variables, the governing equations can be expressed in non-dimensional form:

$$\nabla^* \bullet V = 0, \tag{4}$$

$$\vec{V} \bullet \nabla^* \vec{V} = -\nabla^* p^* + Pr\nabla^{*2}\vec{V} - \frac{Gr \cdot Pr^2}{Ar^3} \cdot \frac{(1-\rho^*)}{\beta \Delta T}, \tag{5}$$

$$V \bullet \nabla^* T^* = \nabla^{*2} T^*, \tag{6}$$

$$\vec{V} \bullet \nabla^* \omega_A^* = \frac{1}{Le}\nabla^{*2}\omega_A^*. \tag{7}$$

The boundary conditions to the above equations (4) to (7) are given as follows:

On the walls ($0 < x^* < L/H$, $y^* = 0$ and 1):

$$u(x^*, 0) = u(x^*, 1) = v(x^*, 0) = v(x^*, 1) = 0 \tag{8}$$

$$\frac{\partial \omega_A^*(x^*, 0)}{\partial y^*} = \frac{\partial \omega_A^*(x^*, 1)}{\partial y^*} = 0,$$

$$T^*(x^*, 0) = -\frac{1}{Ar} \cdot x^* + 1$$

On the source ($x^* = 0$, $0 < y^* < 1$):

$$u(0, y^*) = -\frac{1}{Le(Cv-1)} \frac{\partial \omega_A^*(0, y^*)}{\partial x^*}, \tag{9}$$

$$v(0, y^*) = 0,$$

$$T^*(0, y^*) = 1,$$

$$\omega_A^*(0, y^*) = 1.$$

On the crystal ($x^* = L/H$, $0 < y^* < 1$):

$$u(L/H, y^*) = -\frac{1}{LeCv} \frac{\partial \omega_A^*(L/H, y^*)}{\partial x^*} \tag{10}$$

$$v(L/H, y^*) = 0,$$

$$T^*(L/H, y^*) = 0,$$

$$\omega_A^*(L/H, y^*) = 0.$$

The numerical investigation utilized the Semi-Implicit Method Pressure-Linked Equations Revised (SIMPLER) [35] iterative technique for the system of non-linear, coupled governing partial differential equations. A 63 x 63 (x x y) and a 43 x 23 (x x y) grid system were used for $Ar = 1$ and $Ar \geq 2$, respectively. The numerical verifications of one's results can be found in references [3, 5, 6].

3. Results and Discussion

Double diffusion convection during the physical vapor transport is computationally investigated. When $M_A \neq M_B$, the two molecular weights of Hg_2Br_2 and argon are different, solutally buoyancy driven convection is important compared with thermally buoyancy driven convection. This case arises when the temperature profile imposed on walls has little effect on the crystal growth rate. As pointed by Duval [30], the double diffusion convection flow fields can be characterized by 7 dimensionless numbers, i.e., solutal Grashof number

Table 1
Typical thermo-physical properties ($M_A = 560.988$, $M_B = 39.944$)

Prandtl number, Pr	0.79
Lewis number, Le	0.78
Peclet number, Pe	4.1
Concentration number, C_v	1.01
Aspect ratio, Ar (length = 2 cm, width = 2 cm)	1
Thermal Grashof number, Gr_t	9.85×10^4
Solutal Grashof number, Gr_s	6.79×10^5

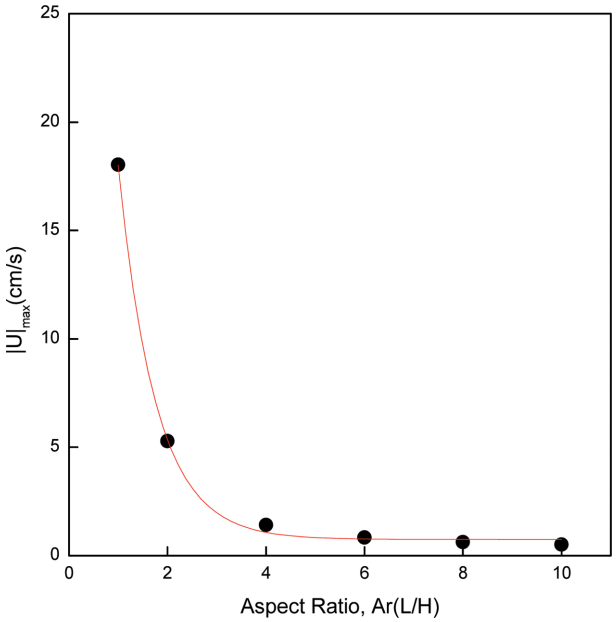

Fig. 2. The $|U|_{max}$ as a function of the aspect ratio, Ar(L/H).

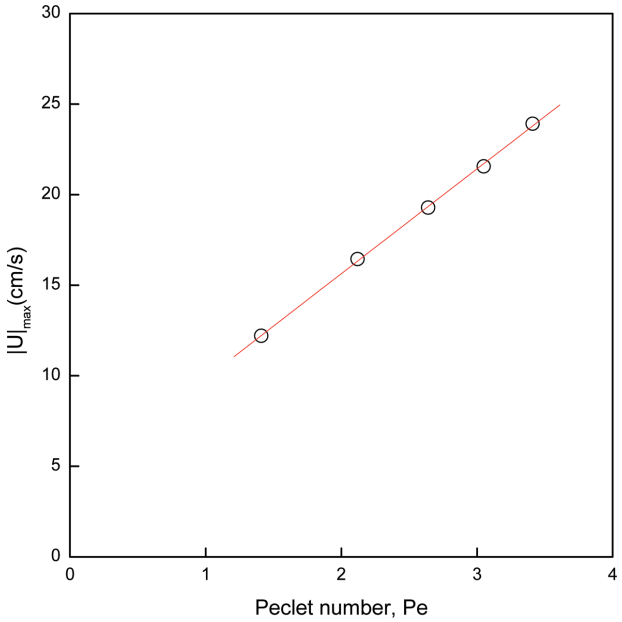

Fig. 3. The $|U|_{max}$ as a function of the dimensionless Peclet number, Pe.

(Gr_s), thermal Grashof number (Gr_t), aspect ratio (Ar), Prandtl number (Pr), Lewis number (Le), concentration number (C_v), and Peclet number (Pe). One's interest is restricted on his study to investigate the relations of maximum magnitudes of velocity vector and double-diffusion convection parameters of aspect ratio, Peclet number and the driving force for the transport of crystal species.

Fig. 2 illustrates the effects of aspect ratio, Ar (L/H) on the dimensional maximum magnitude of velocity vector, $|U|_{max}$, for various aspect ratio, $1 \le Ar \le 10$, based on $\Delta T = 30^oC$ ($290^oC \rightarrow 260^oC$), and 1 g_0, one gravity vector, $P_B = 10$ Torr, $Pr = 0.99$, $Le = 0.15$, $C_v = 1.31$, $Pe = 1.4$, $Gr_t = 2.26 \times 10^3$, $Gr_s = 3.87 \times 10^4$. As shown in Fig. 2, $|U|_{max}$ diminishes first order exponentially with the aspect ratio, $1 \le Ar \le 10$. This trend is an agreement with the previous results [34]. For the range of $1 \le Ar \le 2$, the $|U|_{max}$ diminishes rapidly, and, for $2 \le Ar \le 10$, dwindles down slowly. In other words, the $|U|_{max}$ decreases much sharply near $Ar = 1$, and, then since $Ar = 2$, decreases. With an increase in the aspect ratio, the side wall effects result in a decrease in the $|U|_{max}$, which is consistent with the previous results [30, 36]. In other words, the side wall effects enhance the viscous force which would alleviate the effects of the convection. As the horizontal narrow cavity approaches to $Ar = 10$, the $|U|_{max}$ decreases due to the side wall effects. Therefore, the aspect ratios of the growth ampoule is proved one of important double-diffusive convection parameters. The $|U|_{max}$ diagram versus the Peclet number is shown in Fig. 3. It is obvious that the relationship of the $|U|_{max}$ versus the Peclet number is directly linear. The Peclet number is associated with the advections across the interfaces at the source and the crystal regions.

Fig. 4 shows the relation of ΔT and $|U|_{max}$ is direct and linear for $10^oC \le \Delta T \le 50^oC$, where the temperature of the source region is fixed at 290^oC, with Ar =

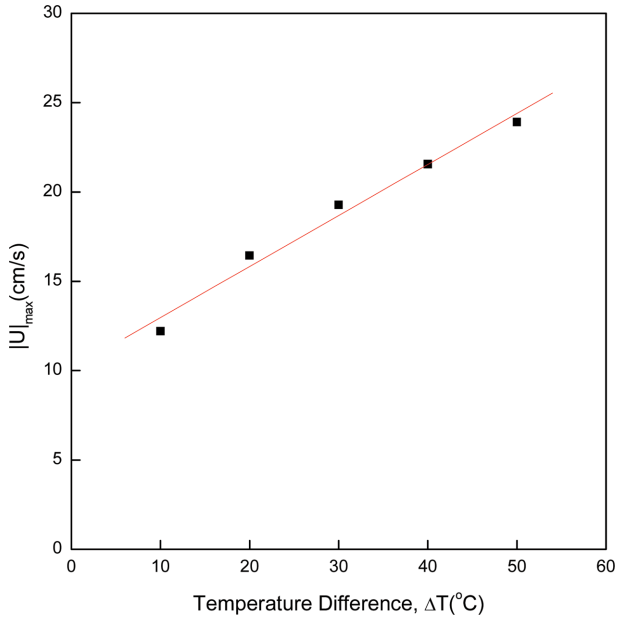

Fig. 4. The $|U|_{max}$ as a function of the temperature difference, ΔT (^oC), Peclet number, Pe, based on $Ar = 1$, $T_s = 290^oC$ fixed, 1 g_0, $P_B = 10$ Torr, $1.8 \times 10^3 \le Gr_t \le 2.9 \times 10^3$, $2.6 \times 10^4 \le Gr_s \le 4.9 \times 10^4$.

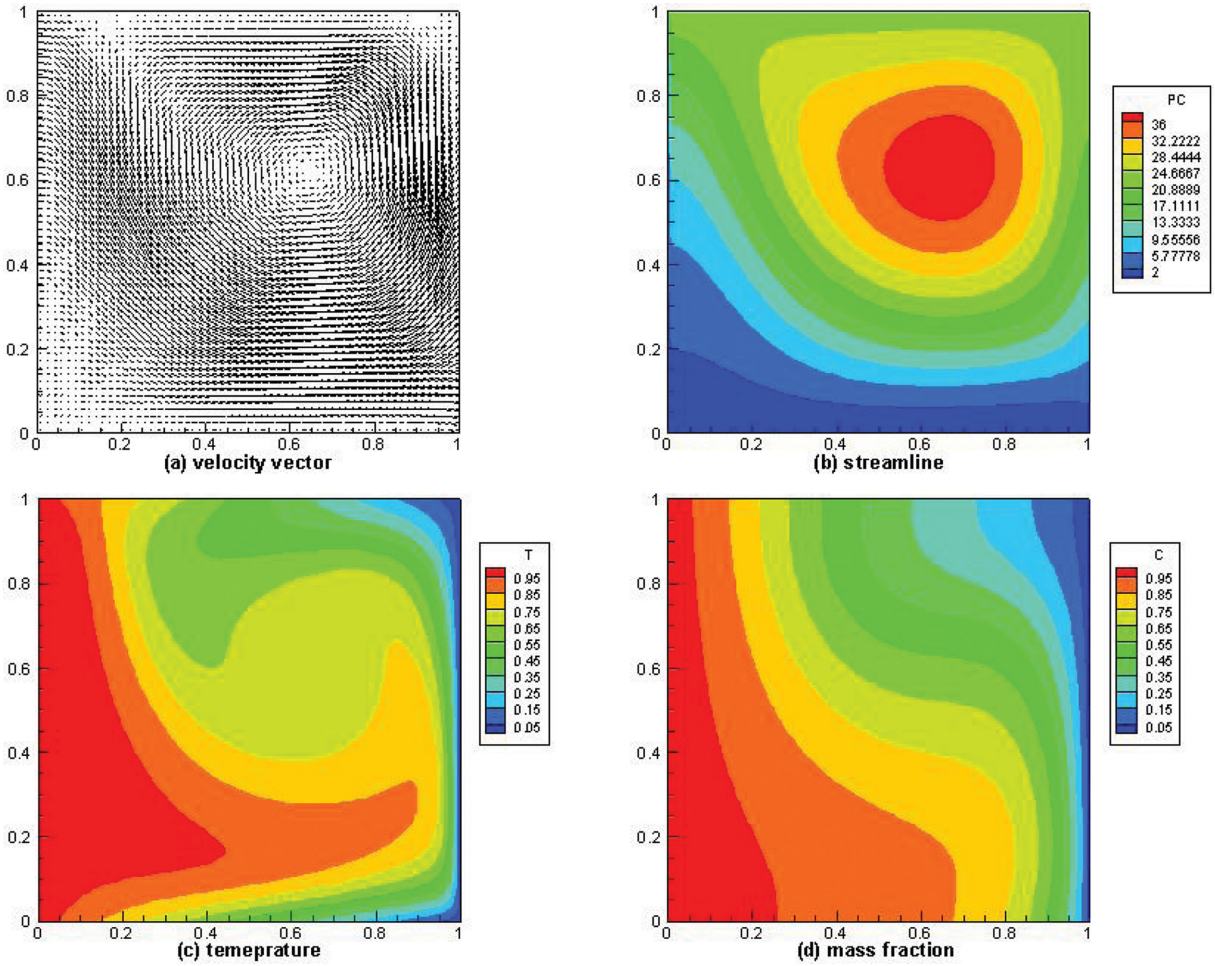

Fig. 5. (a) Velocity vector profile, (b) streamline profile, (c) temperature profile, (d) mass fraction profile, based on Ar = 1, ΔT = 20°C (290°C → 270°C), 1 g_0, P_B = 10 Torr, Pr = 0.99, Le = 0.18, C_v = 1.13, Pe = 2.12, $Gr_t = 2.9 \times 10^3$, $Gr_s = 4.9 \times 10^4$. $|U|_{max}$ = 16.44 cm s^{-1}.

1, 1 g_0, P_B = 10 Torr, $1.8 \times 10^3 \le Gr_t \le 2.9 \times 10^3$, $2.6 \times 10^4 \le Gr_s \le 4.9 \times 10^4$. This relation illustrates that the temperature difference, as the driving force of physical vapor transport causes always thermally buoyancy driven convection through the density gradient associated with the gravity vector. Fig. 5 shows velocity vector, streamline, temperature, mass fraction profiles, based on Ar = 1, ΔT = 20°C (290°C → 270°C), 1 g_0 and P_B = 10 Torr, $|U|_{max}$ = 16.44 cm s^{-1}. As plotted in Fig. 5, there exists single convective roll in the vapor phase, and the flow pattern is asymmetrical against at x^* = 0.5 and three-dimensional flow structure. Convection roll is positioned to the right crystal region wall and the upper wall. As shown in Fig. 5(d), the intervals of mass fraction exhibit close spacings, which indicates the diffusion-limited mass transfer.

Fig. 6 shows the effects of gravity accelerations on $|U|_{max}$ for 10^{-5} $g_0 \le g_y \le 10$ g_0, based on Ar = 1, ΔT = 50°C (290°C → 240°C), P_B = 10, Pr = 0.97, Le = 0.37, C_v = 1.03, Pe = 3.41. The solutally dominant convec-

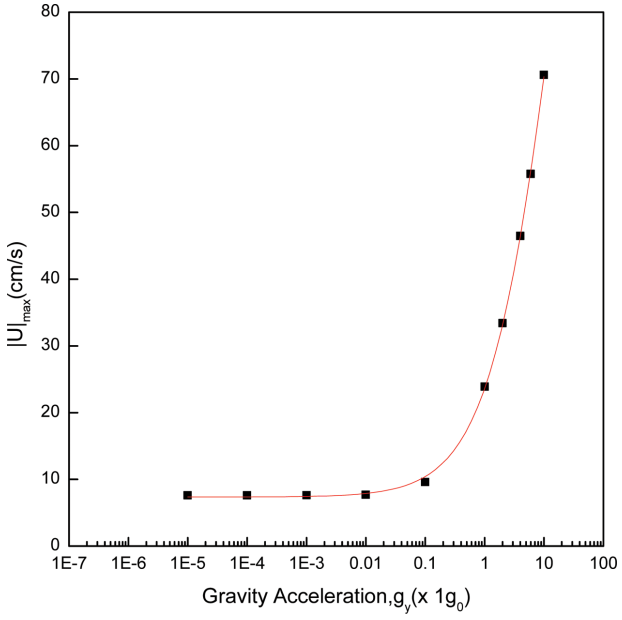

Fig. 6. $|U|_{max}$ as a function of gravity accelerations, 10^{-5} $g_0 \le g_y \le 10$ g_0, based on Ar = 1, ΔT = 50°C (290°C → 240°C), P_B = 10, Pr = 0.97, Le = 0.37, C_v = 1.03, Pe = 3.41.

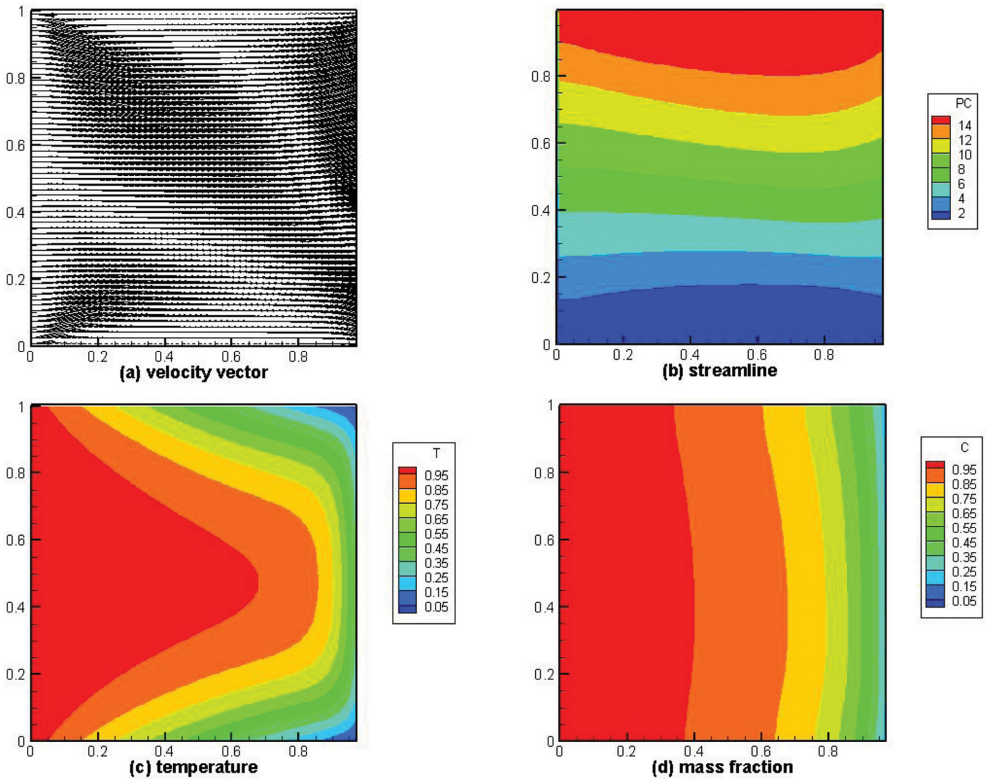

Fig. 7. (a) Velocity vector profile, (b) streamline profile, (c) temperature profile, (d) mass fraction profile, based on Ar = 1, $\Delta T = 50^{\circ}C$ ($290^{\circ}C \rightarrow 240^{\circ}C$), 10^{-2} g_0, $P_B = 10$ Torr, Pr = 0.97, Le = 0.37, $C_v = 1.03$, Pe = 3.41, $Gr_t = 1.8 \times 10^1$, $Gr_s = 2.6 \times 10^2$. $|U|_{max} = 7.7$ cm s^{-1}.

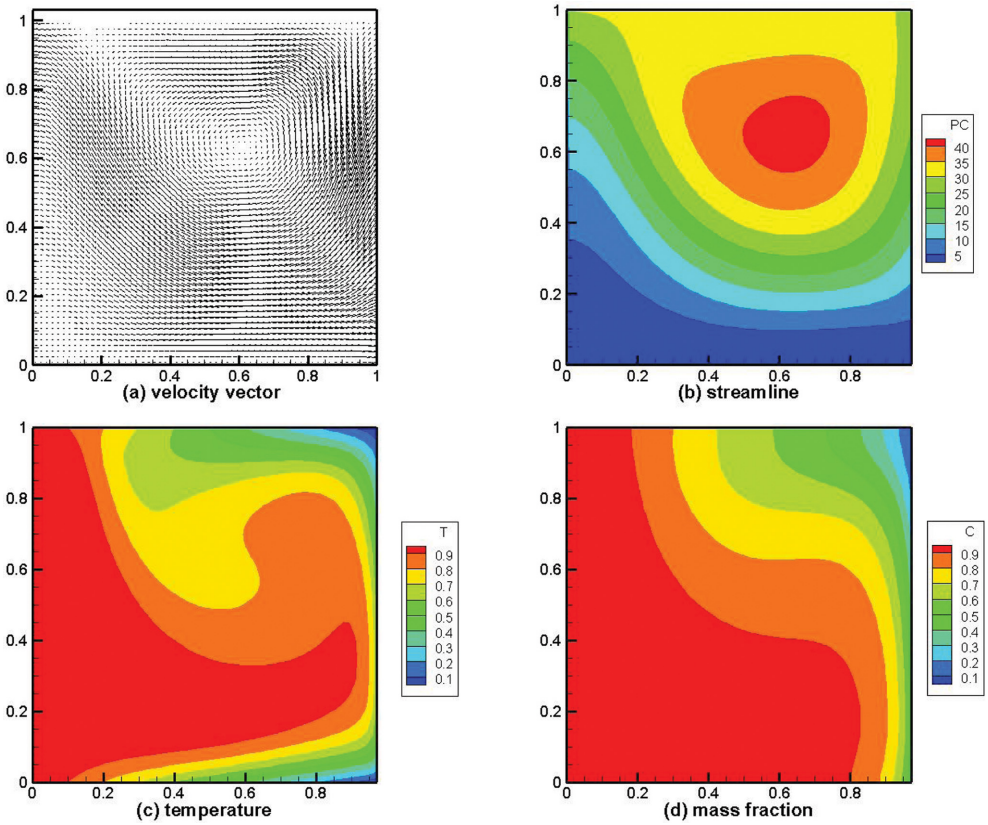

Fig. 8. (a) Velocity vector profile, (b) streamline profile, (c) temperature profile, (d) mass fraction profile, based on Ar = 1, $\Delta T = 50^{\circ}C$ ($290^{\circ}C \rightarrow 240^{\circ}C$), 1 g_0, $P_B = 10$ Torr, Pr = 0.97, Le = 0.37, $C_v = 1.03$, Pe = 3.41, $Gr_t = 1.8 \times 10^3$, $Gr_s = 2.6 \times 10^4$. $|U|_{max} = 23.91$ cm s^{-1}.

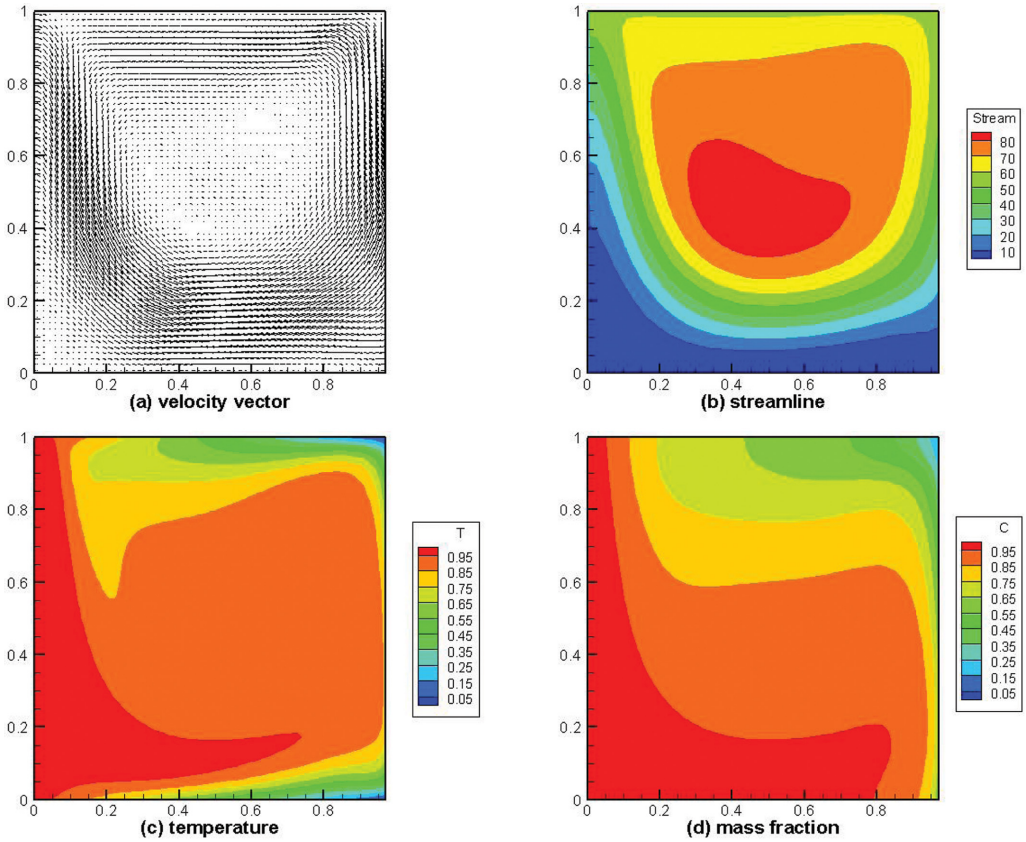

Fig. 9. (a) Velocity vector profile, (b) streamline profile, (c) temperature profile, (d) mass fraction profile, based on Ar = 1, $\Delta T = 50^{\circ}C$ ($290^{\circ}C \rightarrow 240^{\circ}C$), 10 g_0, $P_B = 10$ Torr, Pr = 0.97, Le = 0.37, $C_v = 1.03$, Pe = 3.41, $Gr_t = 1.8 \times 10^4$, $Gr_s = 2.6 \times 10^5$. $|U|_{max} = 70.60$ cm s^{-1}.

tion mode is predominant over the diffusion mode for 10^{-1} $g_0 \le g_y \le 10$ g_0. The solutally dominant convection mode is transited into the diffusion mode at $g_y = 0.1$ g_0 and, since $g_y = 0.1$ g_0, down to $g_y = 10^{-4}$ g_0, the diffusion becomes predominant. As seen in Fig. 6 $|U|_{max}$ drop sharply for 10^{-1} $g_0 \le g_y \le 10$ g_0. This indicates the mass transport is diffusion-dominated under gravity environments less than 0.1 g_0. One can see that the effect of solutally buoyancy driven convection is first important and then decreases rapidly and eventually the mode of transport becomes largely diffusion. Therefore, the parameter of the gravity vector is much important so that it could provide the researchers related to μg environments much motivations to perform numerical studies under μg environments.

Figs. 7 through 9 show velocity vector, streamline, temperature, mass fraction profiles, based on Ar = 1, $\Delta T = 50^{\circ}C$ ($290^{\circ}C \rightarrow 240^{\circ}C$), $P_B = 10$ Torr, Pr = 0.97, Le = 0.37, $C_v = 1.03$, Pe = 3.41 for three different gravities of 10^{-2} g_0, 1 g_0 and 10 g_0. Figs. 7, 8 and 9 are related to 10^{-2} g_0, 1 g_0 and 10 g_0, respectively. The corresponding $|U|_{max}$ s are 7.7 cm s^{-1}, 23.91 cm s^{-1}, 70.60 cm s^{-1}, respectively. With increasing the magnitude of the gravity vector from 10^{-2} g_0 to 1 g_0 by two order of magnitude, the corresponding $|U|_{max}$ is increased by a factor of 3, whereas increasing the magnitude of the gravity vector from 1 g_0 to 10 g_0 by one order of magnitude, the corresponding $|U|_{max}$ is increased by a factor of 2.

4. Conclusions

It is concluded that the $|U|_{max}$ diminishes first order exponentially with the aspect ratio, $1 \le Ar \le 10$. For the range of $1 \le Ar \le 2$, the $|U|_{max}$ diminishes rapidly, and, for $2 \le Ar \le 10$, dwindles down slowly. In other words, the $|U|_{max}$ decreases much sharply near Ar = 1, and, then since Ar = 2, decreases. The μg conditions less than 10^{-2} g make the effect of double-diffusion convection much reduced so that adequate advective-diffusion mass transfer could be obtained.

Acknowledgement

This work was supported by 2019 Hannam Univer-

sity Research Fund (Project No. 2019A172, research period of April 1, 2019 through March 31, 2020).

References

[1] S. Ostrach, "Fluid Mechanics in crystal growth- The 1982 Freeman Scholar Lecture", J. Fluids Eng. 105 (1983) 5.
[2] W.T. Lai, "Natural heat and mass transfer in a rectangular enclosure", Ph.D. Thesis, The University of Minnesota, December 1988.
[3] G.T. Kim, W.M.B. Duval, M.E. Glicksman and N.B. Singh, "Thermal convective effects on physical vapor transport growth of mercurous chloride (Hg_2Cl_2) crystals for axisymmetric 2D cylindrical enclosure", Modelling Simul. Mater. Sci. Eng. 3 (1995) 331.
[4] G.T. Kim, J.T. Lin, O.C. Jones, M.E. Glicksman, W.M. B. Duval and N.B. Singh, "Effects of convection during the physical vapor transport process: application of laser Doppler velocimetry", J. Cryst. Growth 165 (1996) 429.
[5] G.T. Kim, W.M.B. Duval and M.E. Glicksman, "Thermal convection in physical vapour transport of mercurous chloride for rectangular enclosures", Modelling Simul. Mater. Sci. Eng. 289 (1997) 289.
[6] G.T. Kim, W.M.B. Duval and M.E. Glicksman, "Effects of asymmetric temperature profiles on thermal convection during physical vapor transport of Hg_2Cl_2", Chem. Eng. Comm. 162 (1997) 45.
[7] G.T. Kim, J.W. Choi, M.O. Lee, M.H. Kwon and S.K. Kwon, "Effect of stabilizing temperature gradients on thermal convection in rectangular Enclosures during physical vapor transport", J. Korean Cryst. Growth Technol. 9 (1999) 94.
[8] S.K. Kim, S.Y. Son, K.S. Song, J.-G. Choi and G.T. Kim, "Mercurous bromide (Hg_2Br_2) crystal growth by physical vapor transport and characterization", J. Korean Cryst. Growth Technol. 12 (2002) 272.
[9] G.T. Kim, "Growth and characterization of lead bromide: application to mercurous bromide", J. Korean Cryst. Growth Technol. 14 (2004) 50.
[10] G.T. Kim and M.H. Kwon, "Lead bromide crystal growth from the melt and characterization: the effects of nonlinear thermal boundary conditions on convection during physical vapor", J. Korean Cryst. Growth Technol. 13 (2004) 187.
[11] G.T. Kim, "Convective-diffusive transport in mercurous chloride (Hg_2Cl_2) crystal growth", J. Ceramic Process. Res. 6 (2005) 110.
[12] G.T. Kim and K.H. Lee, "Effect of aspect ratio on solutally buoyancy-driven convection in mercurous chloride (Hg_2Cl_2) crystal growth processes", J. Korean Cryst. Growth Technol. 16 (2006).
[13] J.G. Choi, K.H. Lee, M.H. Kwon and G.T. Kim, "Effect of accelerational perturbations on physical vapor transport crystal growth under microgravity environments", J. Korean Cryst. Growth Technol. 16 (2006) 203.
[14] G.T. Kim, K.H. Lee and J.G. Choi, "Essence of thermal convection for physical vapor transport of mercurous chloride in regions of high vapor pressure", J. Korean Cryst. Growth Technol. 17 (2007) 231.
[15] J.G. Choi, K.H. Lee and G.T. Kim, "Ground-based model study for spaceflight experiments under microgravity environments on thermo-solutal convection during physical vapor transport of mercurous chloride", J. Korean Cryst. Growth Technol. 17 (2007) 256.
[16] J.G. Choi, K.H. Lee and G.T. Kim, "Effects of inert gas (Ne) on thermal convection of mercurous chloride system of Hg_2Cl_2 and Ne during physical vapor transport", J. Korean Cryst. Growth Technol. 18 (2008) 225.
[17] J.G. Choi, K.H. Lee and G.T. Kim, "Generic studies on thermo-solutal convection of mercurous chloride system of Hg_2Cl_2 and Ne during physical vapor transport", J. Korean Cryst. Growth Technol. 19 (2009) 39.
[18] G.T. Kim and M.H. Kwon, "Theoretical gravity studies on roles of convection in crystal growth of Hg_2Cl_2-Xe by physical vapor transport under normal and high gravity environments", J. Korean Cryst. Growth Technol. 19 (2009) 107.
[19] J.G. Choi, M.H. Kwon and G.T. Kim, "Effects of total pressure and gravity level on the physical vapor transport of Hg_2Cl_2-Cl_2 system", J. Korean Cryst. Growth Technol. 19 (2009) 116.
[20] G.T. Kim, M.H. Kwon and K.H. Lee, "Effects of thermal boundary conditions and microgravity environments on physical vapor transport of Hg_2Cl_2-Xe system", J. Korean Cryst. Growth Technol. 19 (2009) 172.
[21] G.T. Kim and Y.J. Kim, "Effects of impurity (N_2) on thermo-solutal convection during the physical vapor transport processes of mercurous chloride", J. Korean Cryst. Growth Technol. 20 (2210) 117.
[22] G.T. Kim and Y.J. Kim, "Influence of thermo-physical properties on solutal convection by physical vapor transport of Hg_2Cl_2-N_2 system: Part I - solutal convection", J. Korean Cryst. Growth Technol. 20 (2010) 125.
[23] G.T. Kim, "Importance of convection during physical vapor transport of Hg_2Cl_2 in the presence of Kr under environments of high gravitational accelerations", J. Korean Cryst. Growth Technol. 22 (2012) 29.
[24] Y.K. Lee and G.T. Kim, "Effects of convection on physical vapor transport of Hg_2Cl_2 in the presence of Kr - Part I: under microgravity environments", J. Korean Cryst. Growth Technol. 23 (2013) 20.
[25] G.T. Kim and M.H. Kwon, "Effects of solutally dominant convection on physical vapor transport for a mixture of Hg_2Br_2 and Br_2 under microgravity environments", Korean Chem. Eng. Res. 52 (2014) 75.
[26] G.T. Kim, "Effects of aspect ratio on diffusive-convection during physical vapor transport of Hg_2Cl_2 with impurity of NO", Appl. Chem. Eng. 26 (2015) 746.
[27] G.T. Kim and M.H. Kwon, "Numerical analysis of the influences of impurity on diffusive-convection flow fields by physical vapor transport under terrestrial and microgravity conditions: with application to mercurous chloride", Appl. Chem. Eng. 27 (2016) 335.
[28] G.T. Kim, "A time dependent thermal and solutal convection problem in physical vapor transport of Hg_2Cl_2-I_2 system", J. Korean Cryst. Growth Technol. 27 (2017) 1.
[29] G.T. Kim and M.H. Kwon, "Convective heat and mass transfer affected by aspect ratios for physical vapor transport crystal growth in two dimensional rectangular

enclosures", J. Korean Cryst. Growth Technol. 28 (2018) 63.
[30] W.M.B. Duval, "Transition to chaos in the physical transport process—I", the Proceeding of the ASME--WAM Winter Annual meeting, Fluid mechanics phenomena in microgravity, ASME-WAM, Nov. 28 -- Dec. 3, New Orleans, Louisiana (1993).
[31] N.B. Singh, M. Gottlieb, A.P. Goutzoulis, R.H. Hopkins and R. Mazelsky, "Mercurous Bromide acousto-optic devices", J. Cryst. Growth 89 (1988) 527.
[32] N.B. Singh, M. Marshall, M. Gottlieb, G.B. Brandt, R.H. Hopkins, R. Mazelsky, W.M.B. Duval and M.E. Glicksman, "Purification and characterization of mercurous halides", J. Cryst. Growth 106 (1990) 61.
[33] P.M. Amarasinghe, J.S. Kim, H. Chen, S. Trivedi, S.B. Qadri, J. Soos, M. Diestler, D. Zhang, N. Gupta and J.L. Jensen, "Growth of high quality mercurous halide sing crystals by physical vapor transport method for AOM and radiation detection applications", J. Cryst. Growth 450 (2016) 96.
[34] S.H. Ha and G.T. Kim, "Preliminary studies on double-diffusive natural convection during physical vapor transport crystal growth of Hg_2Br_2 for the spaceflight experiments", Korean Chem. Eng. Res. 57 (2019) 289.
[35] S.V. Patankar, Numerical Heat Transfer and Fluid Flow, Hemisphere Publishing Corp., Washington D. C. (1980).
[36] I. Catton, "Effect of wall conducting on the stability of a fluid in a rectangular region heated from below", J. Heat Transfer 94 (1974) 446.
[37] A. Nadarajah, F. Rosenberger and J. Alexander, "Effects of buoyancy-driven flow and thermal boundary conditions on physical vapor transport", J. Cryst. Growth 118 (1992) 49.